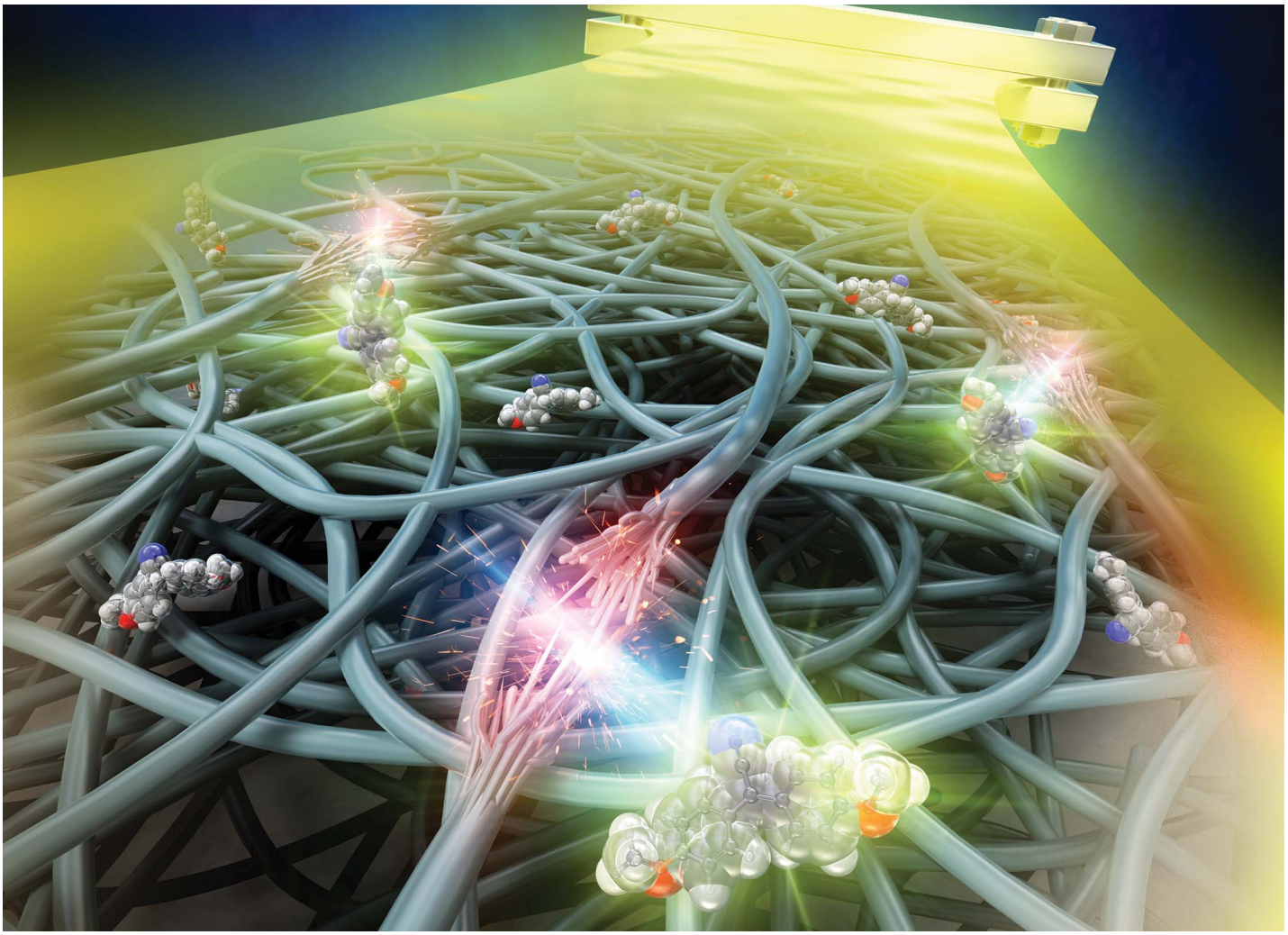

Showcasing research from Professor Otsuka's laboratory, School of Chemical Science and Engineering, Tokyo Institute of Technology, Japan.

Visualization of mechanochemical polymer-chain scission in double-network elastomers using a radical-transfer-type fluorescent molecular probe

The fracture phenomena in Double-network (DN) elastomers are much less understood than those in DN gels due to the limited scope of visualization methods. Here, we demonstrate the visualization of sacrificial bond cleavage in DN elastomers during elongation by adding a diarylacetonitrile (**DAAN**) derivative as a radical-transfer-type fluorescent molecular probe, which enables the visualization of polymer-chain scission without altering the mechanical properties. A tensile test of the DN elastomers that contain **DAAN** revealed that mechanoradicals are generated from the entire elongated region of the elastomers in the strain-hardening region.

As featured in:

See Takumi Yamamoto *et al.*, *RSC Mechanochem.*, 2024, **1**, 63.

ROYAL SOCIETY OF CHEMISTRY

rsc.li/RSCMechanochem

Registered charity number: 207890

RSC Mechanochemistry

ROYAL SOCIETY OF CHEMISTRY

PAPER

View Article Online
View Journal | View Issue

Cite this: *RSC Mechanochem.*, 2024, **1**, 63

Visualization of mechanochemical polymer-chain scission in double-network elastomers using a radical-transfer-type fluorescent molecular probe†

Takumi Yamamoto, [a] Akira Takahashi[a] and Hideyuki Otsuka *[ab]

Received 8th November 2023
Accepted 5th January 2024

DOI: 10.1039/d3mr00016h

rsc.li/RSCMechanochem

Double-network (DN) elastomers are renowned for combining stiffness and toughness. Their exceptional physical properties have garnered significant attention in recent years. However, the fracture phenomena in DN elastomers are much less understood than those in DN gels due to the limited scope of visualization methods. Here, we demonstrate the visualization of sacrificial bond cleavage in DN elastomers during elongation by adding a diarylacetonitrile (**DAAN**) derivative as a radical-transfer-type fluorescent molecular probe, which enables the visualization of polymer-chain scission without altering the mechanical properties. A tensile test of the DN elastomers that contain **DAAN** revealed that mechanoradicals are generated from the entire elongated region of the elastomers in the strain-hardening region. In contrast, DN gels generate mechanoradicals only at the necked region. This method is expected to accelerate the investigation of the fracture properties of various DN elastomers.

Introduction

The double-network (DN) method is an effective and widely used approach to enhance the toughness of polymeric materials, and has been successfully applied to numerous hydrogel and elastomer systems.[1–6] A comprehensive examination of the fracture mechanisms in DN gels and elastomers is important not only from a fundamental chemical point of view, but also from an application perspective, as it has the potential to propel the development of advanced functional materials. However, analysing the fracture phenomena in polymeric materials still poses a significant challenge due to the short lifetime of the mechanoradicals generated by polymer-chain scission,[7] which makes them difficult to detect even using specialized equipment.[8,9] In the solution, mechanoradicals can be detected using spin-trapping agents, such as nitroso species,[10–17] nitrones,[18] and hydrazyl radicals.[19–21] In DN hydrogels, the mechanoradicals generated by the cleavage of the sacrificial polymer chains can be visualized by using the Fenton reaction,[22] a combination of mechanoradical-induced polymerization and an environment-responsive fluorescent probe,[23] or the use of prefluorescent probes for detecting oxygen-relay radical-trapping reactions.[24] The results of these pioneering studies have greatly advanced research into the fracture and toughening mechanisms of DN hydrogels. However, these mechanoradical-visualization methods theoretically require the presence of water and/or dissolved oxygen in water, and thus cannot be directly applied to DN elastomer systems. Therefore, color-changing mechanophores, which are known as mechanochromophores, have been used to visualize sacrificial bond cleavage in DN elastomers.[4,25–28] Mechanochromophores are molecules wherein chemoselective rearrangements proceed accompanied by optical changes in response to mechanical stress.[29–33] As such, they are ideal tools to obtain crucial information on sacrificial bonds by virtue of their self-reporting capability.[34–37] However, introducing mechanophores into elastomers alters the properties of the original materials, as the activation energy of mechanophores is typically lower than those for the cleavage of representative C–C bonds, which means that the results may not accurately reflect the intrinsic properties of the DN elastomers.[38,39] Moreover, covalent introduction of mechanophores often complicates the synthetic process.

Against this background, we propose here a simple and versatile strategy to evaluate polymer-chain scission in DN elastomers using a radical-transfer-type fluorescent molecular probe that can detect mechanoradicals without affecting the physical properties of the elastomers. For this purpose, we chose a diarylacetonitrile (**DAAN**) derivative with a methoxy group at the *para*-position of the aromatic rings as the fluorescent molecular probe, because it can be easily synthesized in large quantities *via* a one-step reaction (Fig. 1a).[40,41] **DAAN** derivatives react with the highly reactive polymeric mechanoradicals generated by mechanical

[a]*Department of Chemical Science and Engineering, Tokyo Institute of Technology, 2-12-1 Ookayma, Meguro-ku, Tokyo 152-8550, Japan. E-mail: otsuka@mac.titech.ac.jp*
[b]*Living Systems Materialogy (LiSM) Research Group, International Research Frontiers Initiative (IRFI), Tokyo Institute of Technology, 4259 Nagatsuta-cho, Midori-ku, Yokohama 226-8501, Japan*

† Electronic supplementary information (ESI) available. See DOI: https://doi.org/10.1039/d3mr00016h

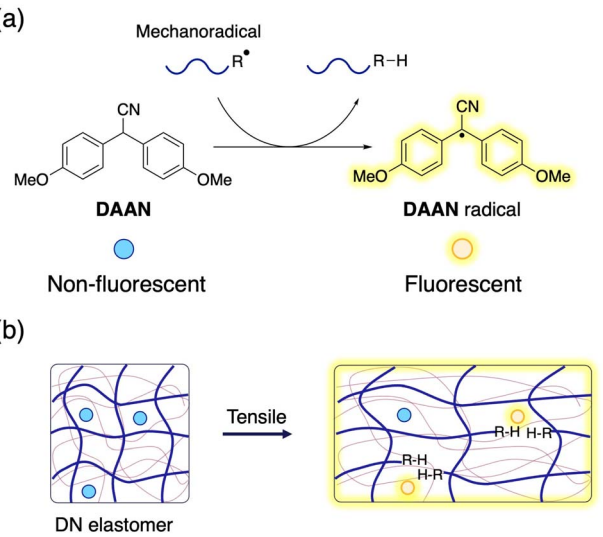

Fig. 1 (a) Chemical reaction of **DAAN** with mechanoradicals. (b) Schematic illustrations of sacrificial bond scission and its visualization using **DAAN** in a DN elastomer.

scission of polymer chains to produce the corresponding **DAAN** radicals,[42,43] which are relatively stable under atmospheric conditions and fluoresce under UV irradiation. As such, **DAAN** is expected to be an ideal probe to obtain information on sacrificial bond cleavage in elastomers without altering their physical properties (Fig. 1b). In addition, the ability to post-synthetically endow DN elastomers with fracture-visualization properties should accelerate the evaluation of their physical properties.

Experimental

Preparation of DN elastomers

The DN elastomers were synthesized according to a previously reported procedure (Fig. 2a).[28] The first networks (FNs) were prepared using ethyl acrylate (EA) and triethylene glycol dimethacrylate (TGD) as cross-linkers *via* free-radical polymerization at room temperature. After washing and drying the resulting films to remove any unreacted components, the obtained FN films were then immersed in a mixture of methyl acrylate (MA), TGD, and the photoinitiator Irgacure 184. The films were swollen to their equilibrium state and then exposed to UV light while maintaining the film temperature <40 °C. Detailed synthetic procedures are provided in the ESI.† We also prepared several DN elastomers with different crosslinker loadings or FN polymer species using the same procedure (Table 1). Here, the weight fraction of the FNs in the DN elastomers varied according to the crosslink density of the FNs. For example, the swelling degree of the FNs in the monomer solution decreases with increasing crosslink density, which in turn led to an increase in the FN weight fraction in the resulting DN elastomers. The detailed properties of the obtained elastomers are summarized in Table S1.†

Then, **DAAN** was incorporated into the synthesized DN elastomers by first swelling them in a saturated solution of **DAAN** in a mixture of chloroform/methanol (1/1, v/v; ~2.46×10^{-2} mol L^{-1}) for 3 h and subsequently shrinking them by immersion in methanol for 3 h (Fig. 2b). The shrunken elastomers were vacuum-dried at 40 °C for 24 h to completely remove the solvent. The thus-prepared **DAAN**-doped elastomers are denoted with the prefix "**DAAN-**". The amount of **DAAN** incorporated was ~1.05 ± 0.15 wt% for all elastomers, as determined by evaluating the weight difference before and after the incorporation process.

Tensile tests

Tensile tests were performed using a SHIMADZU EZ-L instrument equipped with a 100 N load cell at room temperature. For the tests dog-bone-shaped pieces were fabricated from the films in accordance with the JIS-7 standard (12 mm × 2 mm gauge section) with a thickness of 0.62–0.78 mm.

Fluorescence spectroscopy

Fluorescence-spectroscopy measurements were carried out using a spectrofluorometer (JASCO FP-8550) between 500 nm and 750 nm.

Results and discussion

Mechanical and mechanofluorescence properties

To investigate the mechanoradical-visualization ability of **DAAN** in the DN elastomers, **DAAN-EA-3/MA** films were uniaxially stretched at 10 mm min^{-1}. As shown in Fig. 3a, the elastomer exhibited yellow emission under UV irradiation ($\lambda_{ex} = 365$ nm). The fluorescence spectrum of **DAAN-EA-3/MA** after the tensile tests was in good agreement with the spectra derived from the DAAN radicals (Fig. 3b).[40,42] These results suggest that mechanoradicals are generated by sacrificial FN cleavage in the DN elastomer during tensile testing, and that the **DAAN** radicals are generated by the radical-transfer reaction between these mechanoradicals and **DAAN**.

Tensile tests of **EA-3/MA** and **DAAN-EA-3/MA** were conducted to evaluate the effect of the addition of **DAAN**, and the results confirmed that **DAAN** does not affect the stress–strain (S–S) curve (Fig. 3c). These results support the idea that the addition of **DAAN** derivatives enables mechanoradical detection in DN elastomers without altering their mechanical properties.

The mechanoradical generation of the prepared **DAAN**-containing DN elastomers was investigated using uniaxial tensile tests under UV irradiation ($\lambda_{ex} = 365$ nm). All measurements were performed three times for each sample, which confirmed the good reproducibility of the S–S curves (Fig. S1†). All samples begin to show yellow emission at a certain strain, which then increases upon applying the tension (*cf. e.g.*, Movie S1†). For the **DAAN-EA/MA** series with different FN crosslink densities, strain-hardening occurs at lower strain for the higher-crosslink-density samples (Fig. 4a). The onset points coincide well with the onset of fluorescence for **DAAN-EA-2/MA** and **DAAN-EA-3/MA** (Fig. 4b), suggesting that the sacrificial bond cleavage occurs after the strain-hardening begins. However, **DAAN-EA-1/MA** only begins to show emission in the latest stage, long after the onset of strain-hardening. This result suggests that the

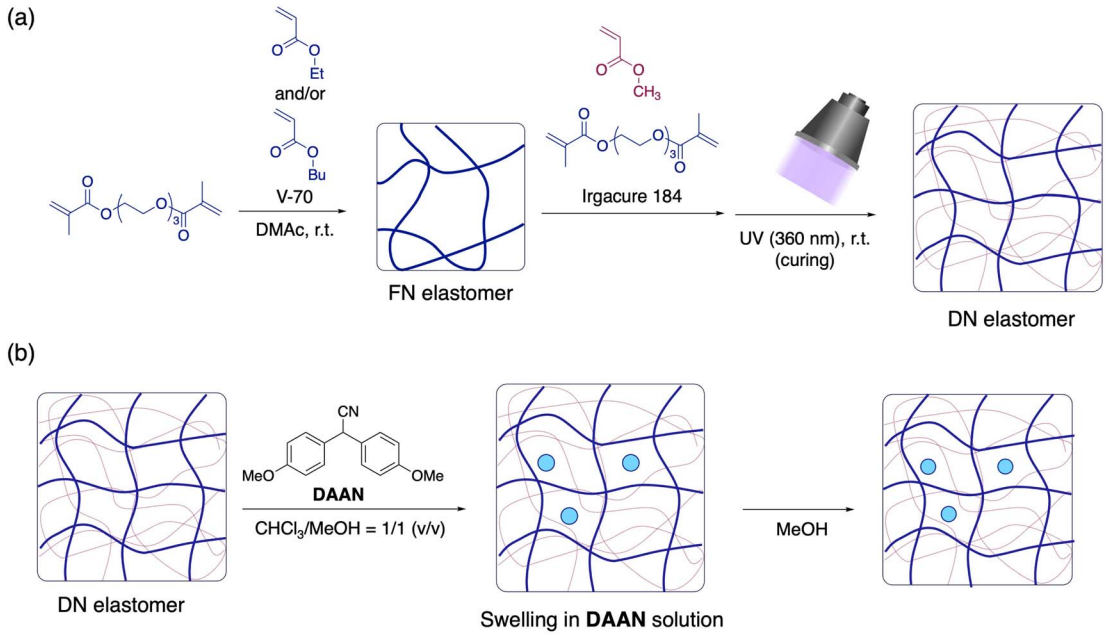

Fig. 2 (a) Synthesis of DN elastomers. (b) Preparation of **DAAN**-containing elastomers (V-70: 2,2′-azobis(4-methoxy-2,4-dimethylvaleronitrile); DMAc: *N*,*N*-dimethylacetamide).

Table 1 Monomer composition and crosslink density of the DN elastomers

		FN		DN	
Entry	Elastomer	Monomer[a]	Crosslink density	Monomer[a]	Crosslink density
1	**EA-1/MA**	EA	1 mol%	MA	1 mol%
2	**EA-2/MA**	EA	2 mol%	MA	1 mol%
3	**EA-3/MA**	EA	3 mol%	MA	1 mol%
4	**BAEA-3/MA**	BA & EA	3 mol%	MA	1 mol%
5	**BA-3/MA**	BA	3 mol%	MA	1 mol%

[a] MA: methyl acrylate; EA: ethyl acrylate; BA: butyl acrylate; BAEA: mixture of BA and EA (1/1, mol/mol).

degree of sacrificial bond cleavage is insufficient to generate **DAAN** radicals at the strain-hardening point in DN elastomers with low crosslink density. In the case of DN gels, it is well established that large numbers of mechanoradicals are generated only in the neck region in the constant-stress regime above the yielding point.[22,24] However, the **DAAN**-doped DN elastomers exhibited fluorescence over almost the entire film. This result indicates that the mechanoradicals are generated over a larger area in the DN elastomers than in the DN gels, and thus suggests a mechanoradical-generation mechanism is different from that of the DN gels. Specifically, the collapse of the first network at a specific area with a concomitant necking event is considered less likely in DN elastomers than in DN gels because of the higher weight fraction of the first network and the friction between the polymer chains during deformation due to the lack of solvent. Consequently, the first network in a DN elastomer is initially elongated without collapse until the strain-hardening point is reached, after which it begins to break over the entire elongated region without necking. In addition, we evaluated the shape recovery of **DAAN-EA-3/MA** after elongating to either 100% or 200% strain, the latter of which exhibited fluorescence due to the polymer chain scission while the former did not. As a result, both specimens fully recovered to their original shapes after the tension was removed irrespective of the chain scission (Fig. S2†). These results suggest that most of the polymer-chain scission in the DN elastomers originated from the first network while little cleavage occurred for the second network that constitutes the majority of the DN elastomer to maintain the overall shape.

Next, we evaluated the effect of the polymer species in the FNs by conducting the same tensile tests on **DAAN-BAEA-3/MA** and **DAAN-BA-3/MA**. As shown in Fig. 4c, their S–S curves were almost identical up to the strain-hardening region, despite the different polymer species in the FN. This is because the mechanical properties up to the strain-hardening region of the DN elastomers are derived from the second network, which accounts for >80% of their mass. Fluorescence was observed starting from the onset of strain-hardening, in the same manner as for **DAAN-EA-3/MA** (Fig. 3d), irrespective of the polymer species in the FN. Interestingly, the fracture stresses and fluorescence intensity at

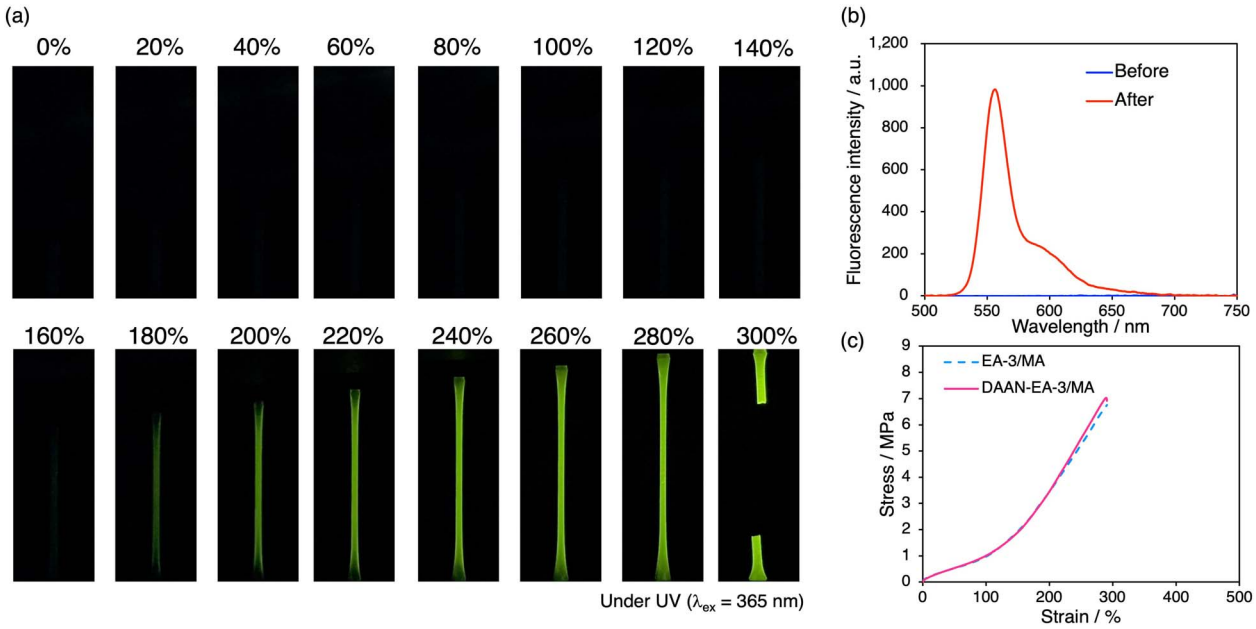

Fig. 3 (a) Digital images of **DAAN-EA-3/MA** during stretching (10 mm min^{-1}) used for fluorescence-intensity analysis. (b) Fluorescence spectra of **DAAN-EA/MA** before and after tensile test. (c) Stress–strain curves of **EA-3/MA** and **DAAN-EA-3/MA**.

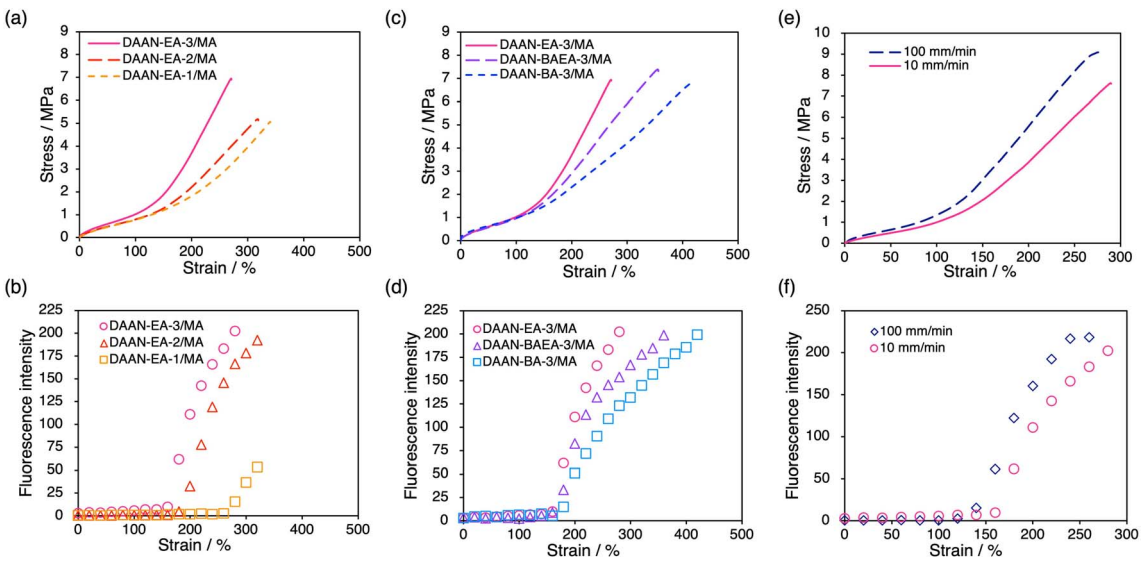

Fig. 4 (a) Stress–strain curves of **DAAN-EA-3/MA**, **DAAN-EA-2/MA**, and **DAAN-EA-1/MA** (10 mm min^{-1}). (b) Fluorescence intensity of **DAAN-EA-3/MA**, **DAAN-EA-2/MA**, and **DAAN-EA-1/MA**. (c) Stress–strain curves of **DAAN-EA-3/MA**, **DAAN-BAEA-3/MA**, and **DAAN-BA-3/MA** (10 mm min^{-1}). (d) Fluorescence intensity of **DAAN-EA-3/MA**, **DAAN-BAEA-3/MA**, and **DAAN-BA-3/MA**. (e) Stress–strain curves of **DAAN-EA-3/MA** (100 mm min^{-1}) and **DAAN-BA-3/MA** (10 mm min^{-1}). (f) Fluorescence intensity of **DAAN-EA-3/MA** (100 mm min^{-1}) and **DAAN-BA-3/MA** (10 mm min^{-1}).

the fracture points are very similar for all the elastomers tested. Since approximately the same amount of **DAAN** is incorporated into each film, the fluorescence intensity should correlate with the amount of mechanoradicals generated. These similarities are likely due to their comparable cross-link densities, which can be expected to result in a similar number of mechanoradicals generated prior to fracture.

To investigate the effect of the strain rate on the fracture behavior of the sacrificial FN, **DAAN-EA-3/MA** was subjected to tensile tests at 100 mm min^{-1}, and the results were compared to those obtained from 10 mm min^{-1}. Strain-hardening occurred earlier in the 100 mm min^{-1} test than in the 10 mm min^{-1} test, and the strain at which the fluorescence emission started was accordingly smaller (Fig. 4e and f). The elastomer properties

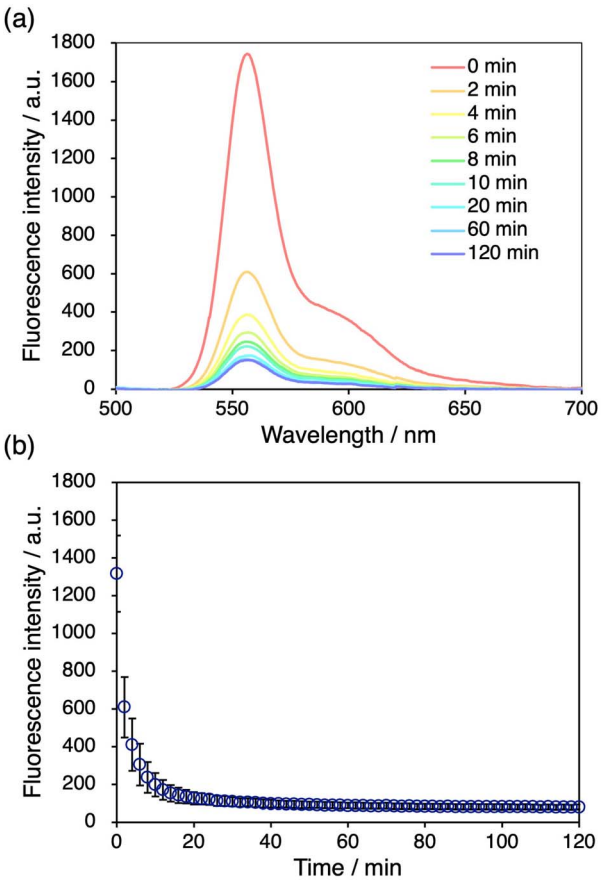

Fig. 5 (a) Time-dependent fluorescence spectra of DAAN-EA/MA after tensile tests. (b) Time-dependent fluorescence intensity at 556 nm after tensile tests.

were further analyzed using Mooney–Rivlin (eqn (1)) plots (Fig. S4 and Table S2†).[44–46]

$$\frac{\sigma}{\left(\lambda - \frac{1}{\lambda^2}\right)} = 2\left(C_1 + \frac{C_2}{\lambda}\right) \quad (1)$$

Here, σ is the stress, λ is the extension ratio, and C_1 and C_2 are the Mooney–Rivlin constants. C_1 is related to the crosslink density while C_2 is related to non-permanent physical crosslinks of the formed network.[47] With increasing tensile speed, the C_1 values decrease while the C_2 values increase. These results indicate that with increasing tensile speed, the polymer chains of the FNs behave like more stretched and the polymer chains become more difficult to untangle. In other words, at higher strain rates, the network shows more elastic behavior and the molecular-chain scission occurs earlier than at slower strain rates, resulting in the **DAAN**-radical-derived fluorescence being observed in the lower-strain region.

Fluorescence decay

We further examined the decay of the fluorescence intensity after stretching the **DAAN**-doped DN elastomers. The fluorescence intensity of the **DAAN-EA-3/MA** films at 556 nm after stretching was monitored over time. We observed that the fluorescence intensity diminished to half of its original value in ~2 min, and that the fluorescence intensity became almost constant after 20 min (Fig. 5). This decay rate is significantly higher than that of **DAAN**-doped polystyrene.[40] We attribute this difference to the higher mobility of the **DAAN** radicals in the elastomeric matrix with a low T_g, considering that **DAAN** radicals generally prefer to dimerize at room temperature.[48] The fast decay hindered our efforts to detect the **DAAN** radicals using electron paramagnetic resonance. However, while the fluorescence intensity decay gradually converged, it did not completely reach zero. This can be interpreted in terms of a diminished probability of the coupling reaction to occur with decreasing concentration of **DAAN** radicals in the DN elastomers. Importantly, such time-dependent emission-quenching properties are advantageous for applications in the spatiotemporal characterization of the fracture of materials.

Conclusions

In summary, we have demonstrated the visualization of sacrificial bond cleavage inside generic DN elastomers by post-synthetically adding a **DAAN** derivative and evaluated the fracture phenomena of the obtained elastomers. Tensile tests showed that sacrificial bond cleavage occurs after the onset of strain-hardening. Increasing the cross-link density of the first network causes the onset strain of mechanoradical generation to decrease and the amount of mechanoradicals generated in the elastomer to increase. Furthermore, very similar fluorescence intensity was observed for elastomers with different acrylate monomers in the first network, indicating that the amount of mechanoradicals generated at rupture is almost identical. Higher strain rates were found to make the network behave more elastically and induce molecular chain scission in the lower-strain region. The present method represents a simple and versatile technique for visualizing covalent bond cleavage in elastomers without altering their physical properties. We expect that these findings will accelerate the elucidation of the fracture mechanisms of elastomers.

Author contributions

T. Y., A. T., and H. O. conceived the concept and designed the experiments. T. Y. performed the experiments and analyzed the data. T. Y., A. T., and H. O. wrote the manuscript.

Conflicts of interest

There are no potential conflicts of interest to declare.

Acknowledgements

This work was supported by KAKENHI grants 21H04689 (to H. O.) from the Japan Society for the Promotion of Science (JSPS), a JSPS Research fellowship for Young Scientists (22J21853 to T. Y.), the ANRI Fellowship (to T. Y.), and JST CREST *via* grant JPMJCR1991 (to H. O.).

Notes and references

1 Q. Chen, H. Chen, L. Zhu and J. Zheng, *J. Mater. Chem. B*, 2015, **3**, 3654–3676.
2 W. Zhang, S. Chen, W. Jiang, Q. Zhang, N. Liu, Z. Wang, Z. Li and D. Zhang, *Eur. Polym. J.*, 2023, **185**, 111807.
3 J. Yang, Y. Li, L. Zhu, G. Qin and Q. Chen, *J. Polym. Sci., Part B: Polym. Phys.*, 2018, **56**, 1351–1362.
4 J. Slootman, V. Waltz, C. J. Yeh, C. Baumann, R. Göstl, J. Comtet and C. Creton, *Phys. Rev. X*, 2020, **10**, 041045.
5 J. Yang, K. Li, C. Tang, Z. Liu, J. Fan, G. Qin, W. Cui, L. Zhu and Q. Chen, *Adv. Funct. Mater.*, 2022, **32**, 2110244.
6 J. P. Gong, Y. Katsuyama, T. Kurokawa and Y. Osada, *Adv. Mater.*, 2003, **15**, 1155–1158.
7 M. K. Beyer and H. Clausen-Schaumann, *Chem. Rev.*, 2005, **105**, 2921–2948.
8 M. Sakaguchi and J. Sohma, *J. Polym. Sci., Polym. Phys. Ed.*, 1975, **13**, 1233–1245.
9 M. Tabata and J. Sohma, *Polym. Degrad. Stab.*, 1979, **1**, 139–154.
10 T. Hayashi, K. Kinashi, W. Sakai, N. Tsutsumi, A. Fujii, S. Inada and H. Yamamoto, *Polymer*, 2021, **217**, 123416.
11 M. Sono, K. Kinashi, W. Sakai and N. Tsutsumi, *Macromolecules*, 2018, **51**, 1088–1099.
12 S. Vivatpanachart, H. Nomura and Y. Miyahara, *Polym. J.*, 1981, **13**, 481–486.
13 M. Sono, K. Kinashi, W. Sakai and N. Tsutsumi, *Macromolecules*, 2017, **50**, 254–263.
14 E. G. Janzen, *Acc. Chem. Res.*, 1971, **4**, 31–40.
15 E. G. Janzen and B. J. Blackburn, *J. Am. Chem. Soc.*, 1968, **90**, 5909–5910.
16 N. J. Bunce, *J. Chem. Educ.*, 1987, **64**, 907.
17 M. Tabata and J. Sohma, *Eur. Polym. J.*, 1980, **16**, 589–595.
18 F. Wang, M. Burck and C. E. Diesendruck, *ACS Macro Lett.*, 2017, **6**, 42–45.
19 S. L. Malhotra, *J. Macromol. Sci., Part A: Pure Appl.Chem.*, 1986, **23**, 729–748.
20 N. Willis-Fox, E. Rognin, C. Baumann, T. A. Aljohani, R. Göstl and R. Daly, *Adv. Funct. Mater.*, 2020, **30**, 2002372.
21 Ö. Laçin, J. Kwiczak-Yiğitbaşı, M. Erkan, Ş. C. Cevher and B. Baytekin, *Polym. Degrad. Stab.*, 2019, **168**, 108945.
22 T. Matsuda, R. Kawakami, R. Namba, T. Nakajima and J. P. Gong, *Science*, 2019, **363**, 504–508.
23 T. Matsuda, R. Kawakami, T. Nakajima and J. P. Gong, *Macromolecules*, 2020, **53**, 8787–8795.
24 Y. Zheng, J. Jiang, M. Jin, D. Miura, F. X. Lu, K. Kubota, T. Nakajima, S. Maeda, H. Ito and J. P. Gong, *J. Am. Chem. Soc.*, 2023, **145**, 7376–7389.
25 E. Ducrot, Y. Chen, M. Bulters, R. P. Sijbesma and C. Creton, *Science*, 2014, **344**, 186–189.
26 H. Zhang, D. Zeng, Y. Pan, Y. Chen, Y. Ruan, Y. Xu, R. Boulatov, C. Creton and W. Weng, *Chem. Sci.*, 2019, **10**, 8367–8373.
27 W. Qiu, P. A. Gurr and G. G. Qiao, *Macromolecules*, 2020, **53**, 4090–4098.
28 T. Watabe, D. Aoki and H. Otsuka, *Macromolecules*, 2022, **55**, 5795–5802.
29 M. A. Ghanem, A. Basu, R. Behrou, N. Boechler, A. J. Boydston, S. L. Craig, Y. Lin, B. E. Lynde, A. Nelson, H. Shen and D. W. Storti, *Nat. Rev. Mater.*, 2021, **6**, 84–98.
30 W. Qiu, J. M. P. Scofield, P. A. Gurr and G. G. Qiao, *Macromol. Rapid Commun.*, 2022, **43**, 2100866.
31 S. Jung and H. J. Yoon, *Synlett*, 2022, **33**, 863–874.
32 M. Xuan, C. Schumacher, C. Bolm, R. Göstl and A. Herrmann, *Adv. Sci.*, 2022, **9**, 2105497.
33 S. Shahi, H. Roghani-Mamaqani, R. Hoogenboom, S. Talebi and H. Mardani, *Chem. Mater.*, 2022, **34**, 468–498.
34 J. Li, C. Nagamani and J. S. Moore, *Acc. Chem. Res.*, 2015, **48**, 2181–2190.
35 N. Willis-Fox, E. Rognin, T. A. Aljohani and R. Daly, *Chem*, 2018, **4**, 2499–2537.
36 Y. Chen, G. Mellot, D. van Luijk, C. Creton and R. P. Sijbesma, *Chem. Soc. Rev.*, 2021, **50**, 4100–4140.
37 M. Stratigaki and R. Göstl, *ChemPlusChem*, 2020, **85**, 1095–1103.
38 Z. Wang, X. Zheng, T. Ouchi, T. B. Kouznetsova, H. K. Beech, S. Av-ron, T. Matsuda, B. H. Bowser, S. Wang, J. A. Johnson, J. A. Kalow, B. D. Olsen, J. P. Gong, M. Rubinstein and S. L. Craig, *Science*, 2021, **374**, 193–196.
39 S. Wang, H. K. Beech, B. H. Bowser, T. B. Kouznetsova, B. D. Olsen, M. Rubinstein and S. L. Craig, *J. Am. Chem. Soc.*, 2021, **143**, 3714–3718.
40 T. Yamamoto and H. Otsuka, *Polym. Chem.*, 2023, **14**, 2464–2468.
41 T. Yamamoto, D. Aoki, K. Mikami and H. Otsuka, *ChemRxiv*, 2023, preprint, DOI: **10.26434/chemrxiv-2023-ss0w5**.
42 T. Yamamoto, S. Kato, D. Aoki and H. Otsuka, *Angew. Chem., Int. Ed.*, 2021, **60**, 2680–2683.
43 T. Yamamoto, D. Aoki and H. Otsuka, *ACS Macro Lett.*, 2021, **10**, 744–748.
44 M. Mooney, *J. Appl. Phys.*, 1940, **11**, 582–592.
45 R. S. Rivlin, *Collected Papers of R. S. Rivlin*, Springer-Verlag, New York, 1997, pp. 90–108.
46 Y. Fukahori and W. Seki, *Polymer*, 1992, **33**, 502–508.
47 G. D. Spathis, *J. Appl. Polym. Sci.*, 1991, **43**, 613–620.
48 T. Sumi, R. Goseki and H. Otsuka, *Chem. Commun.*, 2017, **53**, 11885–11888.